Analyst

Cite this: *Analyst*, 2012, **137**, 4119

www.rsc.org/analyst

COMMUNICATION

Label-free molecular analysis of live *Neospora caninum* tachyzoites in host cells by selective scanning Raman micro-spectroscopy†

Kenny Kong,[a] Christopher J. Rowlands,[a] Hany Elsheikha[b] and Ioan Notingher*[a]

Received 16th May 2012, Accepted 19th July 2012
DOI: 10.1039/c2an35640f

A selective scanning method was used to measure spatially resolved Raman spectra of live *Neospora caninum* tachyzoites colonizing human brain microvascular-endothelial cells. The technique allowed the detection of nucleic acids, lipids and proteins linked to the parasites and their cellular micro-environment at ~10× shorter acquisition time compared to raster scanning.

A key challenge when studying individual living cells is how to extract meaningful spatial and temporal molecular information at a sub-cellular and organelle level without disturbing the cell. Such measurements are crucially important because all biological processes involve highly orchestrated, complex time-dependent molecular interactions. Despite the broad range of techniques available for molecular analysis of cells, such as mass spectrometry,[1] super-resolution immuno-fluorescence imaging[2] or single-cell gene expression,[3] most of them require labelling, fixation, lysis or other invasive procedures. Therefore, these techniques provide only single time-shots of the cells as they cannot measure dynamic molecular events in living cells.[4] Thus, investigations of time-dependent processes often rely on measurements on parallel cell cultures, in which different cells are observed at different time points. One limitation of this approach is that only average quantities can be obtained while important processes caused by the heterogeneity in gene/protein expression or cell cycle may be missed.[5] Transgenic strategies to express markers from specific promoters, such as green fluorescent protein, have been developed to allow time-lapse investigations of live cells with a high level of spatial resolution, but such genetic manipulations require laborious protocols, which may also interfere with the normal behaviour of cells.

Raman micro-spectroscopy (RMS) is a well-established analytical technique which enables label-free chemical analysis of individual cells with micrometric spatial resolution.[6–13] One of the key features of RMS is the ability to perform non-invasive repeated measurements on individual live cells maintained in physiological conditions.[10,14,15] However, the main limitation of CRM is that under non-resonant conditions, most biological molecules have low Raman scattering cross sections. For typical acquisition times of ~1 second per pixel, the conventional raster-scanning method commonly used to collect spatially resolved Raman spectra from cellular structures, the total acquisition time of a Raman map of a cell is ~1 hour. However, in many cases the focus of the study is not on an entire cell but only on a particular part or structure of the cell. In such studies the number of sampling points could be considerably reduced by using more flexible scanning techniques to allow a higher sampling density at the regions of interest and a lower density at the other parts of the cells. In this way the acquisition times could be drastically reduced without compromising the spatial and spectral accuracy of the measurements at the regions of interest.

Recently, a new method for selective scanning has been proposed, in which the sampling points are not selected in a raster fashion but are determined during the measurement based on the spatial and chemical properties of the sample.[16] This sampling algorithm uses two methods to interpolate the previously measured points and the position of the next sampling point corresponds to the position of maximum difference between the two interpolated surfaces. A schematic description of the algorithm is included in the ESI, Fig. S1.†

In this proof-of-principle study we show that selective scanning can be used to significantly reduce the time needed to measure spatially resolved Raman spectra of the protozoan parasite *Neospora caninum* within individual live brain microvascular endothelial cells cultured *in vitro*. *N. caninum* is an obligatory intracellular protozoan, which causes abortion in cattle and neuromuscular diseases in dogs.[17] Label-free molecular analysis of live parasites during infection of host cells at a time-resolution of only few minutes could provide new insight into the molecular mechanisms of the disease, offering new opportunities for more effective therapeutic interventions. The main objective of the study is to use the selective scanning technique to identify the location of the parasites inside the endothelial cells and to ensure appropriate spectral sampling of the parasites and their micro-environment while minimising the total acquisition time.

A schematic description of the Raman micro-spectrometer is included in the ESI, Fig. S2.† The acquisition time for the Raman measurements was 1 second per pixel and the laser power was 170 mW at the sample. At these laser powers and irradiation time, studies on other live cell types indicated that no laser damage was induced to the cells.[10,11,18,19]

Full details on the growth conditions of the human brain micro-vascular endothelial cells (HBMECs) and *Neospora caninum* are included in the ESI.† For Raman measurements, the cells and

[a]*School of Physics and Astronomy, University of Nottingham, Nottingham, NG7 2RD, UK. E-mail: ioan.notingher@nottingham.ac.uk*
[b]*School of Veterinary Medicine and Science, University of Nottingham, Nottingham, LE12 5RD, UK*

† Electronic supplementary information (ESI) available. See DOI: 10.1039/c2an35640f

individual parasites were grown in purpose-built cell chambers.[11,14] At the end of the Raman measurements, the infected HBMECs were fixed in 4% paraformaldehyde in phosphate-buffered saline (PBS, 8.475 g NaCl, 1.093 g Na_2HPO_4, and 0.276 g NaH_2PO_4 in 1 L DI water; pH 7.4) for 30 min or methanol/acetone (1 : 1) for 10 min. Acridine orange was used to stain the nucleus of the cells and the nuclei of individual parasites. The parasites can be identified from the shape, and their small nuclei. The fluorescence images were used to evaluate the ability of the selective sampling algorithm to locate the positions of the parasites inside the host cells. The measurements were carried out on 10 individual *N. caninum*, 10 fixed HBMECs infected with *N. caninum*, and 3 live HBMECs infected with *N. caninum*.

Raman spectral maps (raster scans at 0.5 μm steps) were measured from *N. caninum* individual live parasites to establish their main spectral bands. The mean Raman spectrum of the *N. caninum* (Fig. 1A) consists of typical bands associated to proteins (1660 cm^{-1} amide I, amide III in the 1200–1320 cm^{-1} region, 1003 cm^{-1} phenylalanine, 1450 cm^{-1} CH_2), nucleic acids (1098 cm^{-1} PO_2^- vibrations, O–P–O stretching in DNA and RNA at 788 cm^{-1} and 813 cm^{-1}) and lipids (1449 cm^{-1} CH_2 bending, 1303 cm^{-1} CH_2 twist, C–C stretch 1050–1080 cm^{-1}).[20] Principal component analysis was performed on all spectral maps of *N. caninum* to establish the main spectral variability between parasites (Fig. 1B and C). The loading of PC1 and PC2 (47.8% and 7.2% variance) and the corresponding score maps suggested that the spectral variations captured by PC1 and PC2 were mainly related to the thickness of the cells. However, PC3 and PC4 (variance below 1%) detected finer molecular variations related to lipids (1449 cm^{-1}, 1303 cm^{-1}) and nucleic acids (1098 cm^{-1}, 788 cm^{-1}).

The efficiency of the selective sampling algorithm can be increased if spectral contrast between the parasites and the other regions of the cell is established. The spectral contrast allows the selective scanning algorithm to identify the locations of the parasites inside the HBMECs, and to ensure that these regions are sampled with sufficient density to resolve a high level of detail.

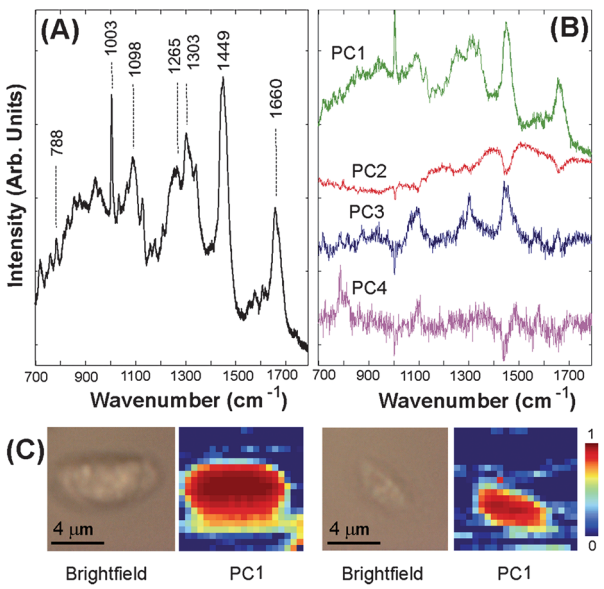

Fig. 1 (A) The mean Raman spectrum of isolated live *Neospora caninum*. (B) The loading of the main principal components (PC1–PC4). (C) Bright field and spectral images (PC1 scores) of two typical *Neospora caninum*.

Spectral maps of HBMECs infected with *N. caninum* for 24 hours were first obtained by raster-scanning. However, since the raster scanning required a long acquisition time (~50 minutes) during which the cells can change their morphology, the measurements were carried out on fixed cells. While several multivariate statistical methods have been reported for increasing the contrast in spectral images of tissues,[21] in this study we used PCA to discriminate individual *N. caninum* in infected HBMECs (Fig. 2A). The loadings of the PC1 and PC3 indicate (Fig. 2B) that the Raman spectra of the parasites were characterised by more intense bands assigned to lipids, particularly the 1449 cm^{-1} and 1303 cm^{-1} bands, compared to their micro-environment, in agreement with Fig. 1A. This finding was supported by a direct comparison between the Raman spectra measured at positions inside the parasite and at a position in its vicinity (Fig. 2C). Since the spectral features used for selective scanning need to be reduced to a scalar so that two interpolation surfaces over the entire sampling area can be obtained, the following scalar value was used in this case:

$$F = (I_{1449} \times I_{1303})/(I_{1265} \times I_{1660})$$

where I_i represents the intensity of the Raman band at wavenumber i.

The intensity of the bands i = 1265, 1303, 1449, and 1660 cm^{-1}, were calculated as the area in the ranges 1255–1275 cm^{-1}, 1290–1310 cm^{-1}, 1385–1534 cm^{-1}, and 1593–1717 cm^{-1}. Fig. 3 presents a typical example of spatially resolved Raman spectra of live *N.*

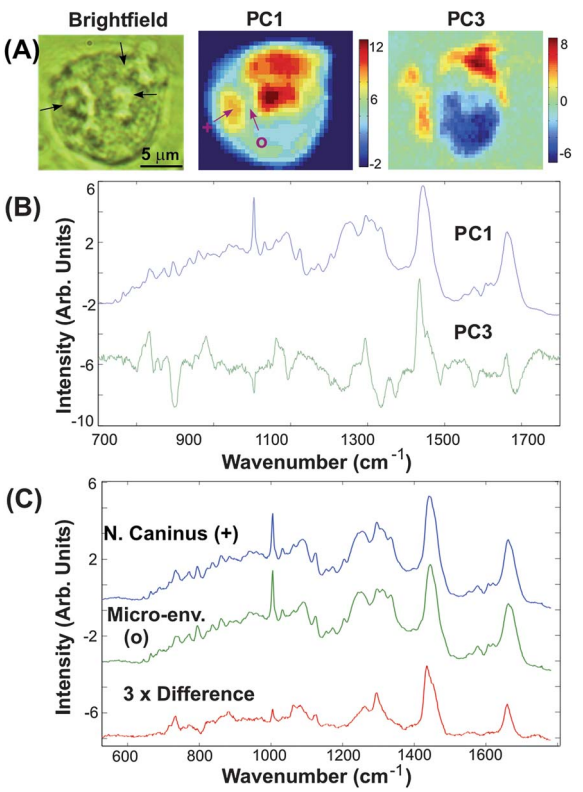

Fig. 2 (A) Bright field image and raster-scan spectral maps (PC1 and PC3 scores) of a typical fixed HBMEC infected with *N. caninum*. The locations of the parasites are indicated by black arrows. (B) PC1 and PC3 loading. (C) Raman spectra (mean over 3 × 3 pixels) at the locations corresponding to a parasite and its micro-environment (positions indicated in (A)) along with the computed difference spectrum.

caninum parasites inside a host HBMEC measured by selective scanning with only 240 sampling points. The fluorescence images obtained after the Raman measurements were used to confirm that the distribution of the sampling points generated by the selective scanning corresponded to the locations of the parasites inside the live cell and focused the sampling points at the infection region (Fig. 3A).

The loadings of PC2 and the maps corresponding to PC2 scores (Fig. 3B) confirmed that the parasites were characterised by intense bands associated with phospholipids. However, further information on the molecular properties of the parasites and their micro-environment was captured by PC3 which showed a spectral band at 1554 cm^{-1}. The map for the PC3 scores indicated that the 1554 cm^{-1} band was more intense at the infection region. Fig. 3C shows spatially resolved Raman spectra from two infected regions of the cell where the selective sampling provided a high sampling density and the

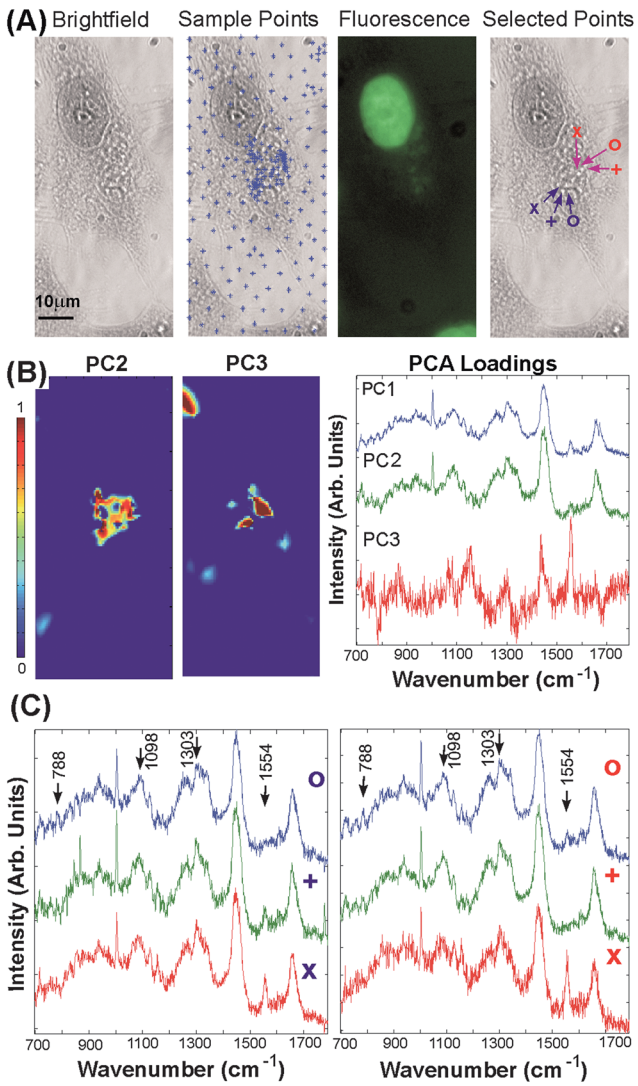

Fig. 3 A typical example of spatially resolved Raman measurements obtained by selective scanning of a live HBMEC infected with *N. caninum*. (A) Bright field image, the distribution of the sampling point, acridine orange fluorescence image and positions of selected Raman spectra for (C). (B) The maps of the PC2 and PC3 scores and the corresponding loadings. (C) Spatially resolved Raman spectra at the positions indicated in (A).

presence of *N. caninum* was confirmed by the fluorescence staining. Although these sampling points were only 2–3 μm apart and the spatial resolution of the instrument was evaluated to ~1.4 μm, the spatially resolved Raman spectra highlight the high molecular heterogeneity of the parasites and their micro-environment. The spectra at the locations indicated by the marks (o) showed Raman bands at 788 cm^{-1} and 1098 cm^{-1} suggesting that these positions corresponded to the parasite nuclei. The regions rich in lipids (intense bands at 1303 cm^{-1} and 1449 cm^{-1}) indicated by the marks (+) can be related to the membranes of the parasites. Raman spectra with an intense band at 1554 cm^{-1} were measured at the infection site (marks x), however it was not clear from the bright-field or fluorescence images whether these locations corresponded to the *N. caninum* or their micro-environment. Since these bands were not detected in the Raman spectra of the live isolated *N. caninum*, it is likely that the band is related to molecules linked to the host–parasite interaction, expressed either by the parasites or by the host cell. Intense bands at 1554 cm^{-1} assigned to tryptophan were reported in the Raman spectra of lysozyme,[22,23] an enzyme associated with the immune response of cells against bacterial and parasite infection. The absence of the 1554 cm^{-1} band in the Raman spectra of the acetone : methanol fixed infected HBMECs may be explained by the fact that lysozyme is soluble in acetone and methanol. However, more detailed studies are required to confirm the assignment of the 1554 cm^{-1} to lysozyme or other tryptophan-rich biomolecules. In addition, the effect of biological variability on the spectral signatures of the infected cells needs to be investigated.[24]

While the selective sampling allowed the acquisition of spatially resolved spectra with approximately 10× shorter acquisition time compared to raster scanning (35 × 80 points at 1 μm step size), it is worthwhile to include a brief discussion on the advantages and limitations of this technique compared to the raster scanning and fluorescence staining imaging. The raster scanning method allows the measurement of all Raman active molecules in the cell without any *a priori* knowledge of the cell and spatial detail limited only by the step-size and the spatial resolution of the microscope. While the selective scanning can focus the sampling to the regions of interest of the cell, it requires some *a priori* knowledge on the sample, in a similar way as fluorescence staining does. However, it is important to note that in comparison to fluorescence imaging, in which the information obtained is limited to the stained molecules, the *a priori* knowledge in selective sampling is used only for determining the sampling positions. Thus, the measured Raman spectra will contain a finger print of all molecules present at the sampled locations. This point is highlighted by the detection of the tryptophan 1554 cm^{-1} band in the Raman spectra measured by the selective sampling, although this band was not used for determining the sampling positions. It is also important to note that if the spectral bands selected for driving the selective sampling are not sufficiently specific to the molecular species of interest, the sampling algorithm becomes less efficient and sampling could be diverted to other cell structures or lead to a non-specific space-filling sampling.

Conclusions

In this paper we have showed that selective sampling can be used to significantly reduce the total acquisition time for spatially resolved Raman spectra of live *N. caninum* within host cells. A high level of spectral and spatial detail was obtained for *N. caninum* tachyzoites and their micro-environment with only 240 sampling points per cell

(4 min total acquisition time), which is equivalent approximately to 10-fold decrease compared to raster scanning. Since the RMS does not require labelling and the cells can be maintained in physiological conditions during the measurements, the reduced acquisition times would make it possible to measure the temporal and spatially resolved molecular changes related to the development of *N. caninum*, as well as the response of the host cells.

Acknowledgements

This paper presents independent research commissioned by the National Institute for Health Research (NIHR) under its Invention for Innovation (i4i) Programme (grant number II-AR-0209-10012). The views expressed are those of the author(s) and not necessarily those of the NHS, the NIHR or the Department of Health.

References

1 P. Sjovall, J. Lausmaa, H. Nygren, L. Carlsson and P. Malmberg, *Anal. Chem.*, 2003, **75**, 3429–3434.
2 B. Huang, H. Babcock and X. Zhuang, *Cell*, 2010, **143**, 1047–1058.
3 F. Tang, C. Barbacioru, S. Bao, C. Lee, E. Nordman, X. Wang, K. Lao and M. A. Surani, *Cell Stem Cell*, 2010, **6**, 468–478.
4 D. G. Spiller, C. D. Wood, D. A. Rand and M. R. H. White, *Nature*, 2010, **465**, 736–745.
5 S. J. Altschuler and L. F. Wu, *Cell*, 2010, **141**, 559–563.
6 G. J. Puppels, F. F. M. Demul, C. Otto, J. Greve, M. Robertnicoud, D. J. Arndtjovin and T. M. Jovin, *Nature*, 1990, **347**, 301–303.
7 A. A. van Apeldoorn, H. J. van Manen, J. M. Bezemer, J. D. de Bruijn, C. A. van Blitterswijk and C. Otto, *J. Am. Chem. Soc.*, 2004, **126**, 13226–13227.
8 Y. S. Huang, T. Karashima, M. Yamamoto and H. Hamaguchi, *Biochemistry*, 2005, **44**, 10009–10019.
9 C. Matthaus, T. Chernenko, J. A. Newmark, C. M. Warner and M. Diem, *Biophys. J.*, 2007, **93**, 668–673.
10 A. Zoladek, F. C. Pascut, P. Patel and I. Notingher, *J. Raman Spectrosc.*, 2011, **42**, 251–258.
11 A. Ghita, F. C. Pascut, M. Mather, V. Sottile and I. Notingher, *Anal. Chem.*, 2012, **84**, 3155–3162.
12 K. Hartmann, M. Becker-Putsche, T. Bocklitz, K. Pachmann, A. Niendorf, P. Rosch and J. Popp, *Anal. Bioanal. Chem.*, 2012, **403**, 745–753.
13 M. Okada, N. I. Smith, A. F. Palonpon, H. Endo, S. Kawata, M. Sodeoka and K. Fujita, *Proc. Natl. Acad. Sci. U. S. A.*, 2012, **109**, 28–32.
14 F. C. Pascut, H. T. Goh, N. Welch, L. D. Buttery, C. Denning and I. Notingher, *Biophys. J.*, 2011, **100**, 251–259.
15 K. Hamada, K. Fujita, N. I. Smith, M. Kobayashi, Y. Inouye and S. Kawata, *J. Biomed. Opt.*, 2008, **13**, 044027.
16 C. J. Rowlands, S. Varma, W. Perkins, I. Leach, H. Williams and I. Notingher, *J. Biophotonics*, 2012, **5**, 220–229.
17 H. M. Elsheikha and N. A. Khan, *Essentials of Veterinary Parasitology*, Caister Academic Press, 2011.
18 A. B. Zoladek, R. K. Johal, S. Garcia-Nieto, F. C. Pascut, A. Ghaemmaghami and I. Notingher, *Analyst*, 2010, **135**, 3205–3212.
19 J. W. Chan, D. K. Lieu, T. Huser and R. A. Li, *Anal. Chem.*, 2009, **81**, 1324–1331.
20 A. T. Tu, *Raman Spectroscopy in Biology: Principles and Applications*, Wiley-Blackwell, 1982.
21 I. I. Patel, J. Trevisan, G. Evans, V. Llabjani, P. L. Martin-Hirsch, H. F. Stringfellow and F. L. Martin, *Analyst*, 2011, **136**, 4950–4959.
22 A. B. Kudryavtsev, S. B. Mirov, L. J. DeLucas, C. Nicolete, M. van der Woerd, T. L. Bray and T. T. Basiev, *Acta Crystallogr., Sect. D: Biol. Crystallogr*, 1998, **54**, 1216–1229.
23 T. Miura, H. Takeuchi and I. Harada, *J. Raman Spectrosc.*, 1989, **20**, 667–671.
24 J. G. Kelly, J. Trevisan, A. D. Scott, P. L. Carmichael, H. M. Pollock, P. L. Martin-Hirsch and F. L. Martin, *J. Proteome Res.*, 2011, **10**, 1437–1448.